Jour. of the KGS, Vol. 20, No. 7. September 2004, pp. 15~24

# GIS-based Loss Estimation and Post-earthquake Assessment of Building Damage

## 빌딩피해에 대한 GIS 손상평가 및 지진 후 평가

Jeon, Sang-Soo[1] 전 상 수


### 요 지

본 논문은 1994 Northridge 지진에 의해 발생된 주거건물손상에 관하여 건물 교체시의 가격에 대한 상대적 수리비용의 개념으로 GIS기반의 손상평가에 관하여 기술하였다. 빌딩손상은 164개의 서로 다른 지역에서 얻어진 지진기록으로부터 유도된 지진매개변수와 빌딩위치 및 안전조사보고서를 바탕으로 평가하였다. 본 논문은 가장 심한 건물피해를 받은 위치를 규명하는 인식 알고리즘이 GIS를 통하여 개발되었다. 이러한 알고리즘은 지진 후 신속한 응급조치와 위성으로부터 얻어진 데이터를 짧은 시간에 분석할 수 있는 프레임을 제공한다.

### Abstract

This paper describes a GIS-based assessment of residential building damage caused by the 1994 Northridge earthquake in which the fractions of existing buildings damaged at various percentages of replacement cost are related to a range of seismic parameters. The assessment uses data from safety inspection reports and tax assessor records, both of which were geocoded and linked to seismic parameters derived from strong motion records at 164 different sites. The paper also describes a GIS-based pattern recognition algorithm for identifying locations of most intense building damage. The algorithm provides a framework for rapidly screening remote sensing data and dispatching emerging services.


**Keywords** : Building damages, Earthquake, Geotechnical engineering, GIS, Seismic parameters

## 1. Introduction

Past earthquakes have shown that economic and social losses are primarily a function of damage to buildings (Kircher, et al., 1997). This is true for two basic reasons: (1) buildings are the predominant kind of facility in the built environments and (2) buildings are vulnerable to earthquake damage. Accurate prediction of building damage and loss is at the heart of reliable estimates of earthquake impacts.

At the time of the 1994 Northridge earthquake, about 90% (over 2 million) of all buildings in Los Angeles County were residential (Kircher, et al., 1997). Estimates of the total cost of the 1994 Northridge earthquake vary from $25.7 billion (Comerio et al., 1996) to $44 billion (Eguchi et al., 1996). About half of these estimates is associated with residential building construction, primarily 1-to 2-story light timber structures. Clearly, residential timber structures play a very important role in the disaster planning and potential earthquake losses of the Los Angeles region.

This paper focuses on the spatial distribution of damage to residential timber buildings caused by the Northridge earthquake. Using safety inspection and tax

1 Member, Chief Researcher, Korea Highway & Transportation Technology, Korea Highway Corporation (ssj3@freeway.co.kr)

assessor records, a GIS database was organized in which the fractions of existing buildings damaged at various percentages of replacement cost were mapped and correlated with a range of seismic parameters derived from 164 strong motion records distributed throughout and adjacent to the San Fernando Valley area (Jeon, 2002). Regressions were developed between timber building damage and various seismic parameters. The most reliable seismic parameters were identified for estimating structural losses. A GIS-based pattern recognition algorithm was developed from the building database for rapid identification of locations of most intense earthquake-related damage. This paper describes the databases, statistical assessments, and GIS analytical process and visualization procedures that have resulted from this work.

## 2. Damage Types of Residential Timber Buildings

Single family residences in the City of Los Angeles range in age from mid-1930's vintage to recent construction and are generally one and two stories in height. Three basic foundation systems are encountered: concrete strip footings, raised perimeter concrete or masonry foundation walls, and concrete slab on grade. The concrete strip footings carry cripple walls that support the floor framing. The raised perimeter concrete or masonry foundation walls and interior posts or raised walls support the first floor framing of the building. The concrete slab-on-grade is integral with the footings.

Safety inspections were performed by teams of structural engineers after the Northridge earthquake. The inspections were performed according to guidelines published by Applied Technology Council (1989). The buildings were tagged according to their hazard to occupants. The tags were categorized according to three different levels of damages and marked with different colors such as red, yellow and green. A red tag was affixed to structures deemed hazardous to life. A yellow tag was assigned to buildings that posed a threat to life, but not so much that an occupant could not re-enter to remove possessions. A green tag was issued to buildings that did not pose a life-safety hazard to the occupants. For most residential structures, these inspections were initiated by calls from the occupants or property owners.

The damage characteristics of residential timber structures and most frequent types of damage were described by Filiatrault and Stieda (1995) and Akers (1994). Extensive damage was observed in the form of collapsed unreinforced brick and stone chimneys and severely racked or collapsed cripple walls.

The cripple wall movements were associated with misplaced, missing, or improperly set anchor bolt or hold-down systems (Akers, 1994). In general, no distress was noted to the sill plate or foundation where anchor bolts were properly installed. Some of the most severe wall movements, however, were observed in newer structures with engineered shear walls and hold-downs. Such damage often occurred where nuts, attaching the anchor bolts to hold-downs, were not in place or were not tightened.

## 3. Loss Estimation Methodology

Past earthquakes have shown that economic and social losses are primarily a function of damage to buildings (Kircher, et al., 1997). This is true for two basic reasons: (1) buildings are the predominant kind of facility in the built environments and (2) buildings are vulnerable to earthquake damage. Accurate prediction of building damage and loss is at the heart of reliable estimates of earthquake impacts.

Los Angeles County had a total population of 8.86 million people and 2.25 million buildings in 1990 (MEGA-CITIES, 2001; Kircher, et al., 1997). About 90% (over 2 million) of all buildings were residential. In terms of replacement cost, residential structures represented about 75% of the total value of all buildings. Residences in Los Angeles County had a replacement cost of $340 billion without contents, or about $510 billion with contents.

Over 99% of all residences were timber frame construction (excluding mobile homes) [Kircher, et al.,

1997]. This percentage applies to single-family residences, which are the most common type of residence. Multi-family residences are primarily timber frame construction, but also include about 5% steel, concrete, or masonry buildings. There are 1.74 million single-family living units (residences) and 1.33 million multi-family living units (in about 230,000 buildings). In rough numbers, single-family residences represent about 75% of the total residential value. These data indicate that light-frame timber buildings are by far the most common type of timber frame building.

By age, about 29% of all residences in Los Angeles were built before 1941, about 65% were built between 1941 and 1976 and about 16% were built after 1976 (Kircher, et al., 1997). In general, damage to residences built before 1941 (i.e., pre-code design level), such as timber frame buildings with cripple walls without bracing or unreinforced masonry (URM) buildings, were much higher than that predicted by modern seismic-code criteria (i.e., moderate-code design level of the FEMA/NIBS methodology).

Estimates of the total cost of the 1994 Northridge earthquake vary from $25.7 billion (Comerio, et al., 1996) to about $44 billion (Eguchi, et al., 1996). The $25.7 billion estimate includes direct economic (i.e., capital-related) loss to public and private property, but does not include indirect economic loss and some amount of direct loss not covered either by insurance or governmental programs. About one-half, $12.7 billion, of the $25.7 billion estimate is associated with residential building reconstruction.

The $44 billion estimate includes direct economic loss, but does not include indirect economic losses. About $24 billion of the $44 billion estimate includes federal and state costs as well as insured losses and costs to repair most damaged lifelines. The sum does not include repair costs outside insurance coverage (e.g., deductibles, costs above insurance limits), and commercial loans to repair damaged structures (Eguchi, et al., 1996). The $44 billion estimate does cover estimates of losses associated with deductibles as well as losses sustained by the 60% of LA homeowners without earthquake coverage.

Private insurance has provided most of the funds for post-Northridge reconstruction. As of June 1996, the California Department of Insurance estimates that the state's private insurance companies have paid a total of about $12.3 billion for Northridge-related claims, of which approximately $9.5 billion, or 78%, has been for residential claims (Kircher, et al., 1997). Insurance claims include four types of coverage: primary structures, appurtenances, contents, and loss of use. Losses of use account for only 5.6% of insurance claims and are not a dominant portion of observed loss.

## 4. Building Damage Database

Inspection records available through the California Office of Emergency Services (OES) were obtained for 62,020 buildings in the San Fernando area that were investigated after the Northridge earthquake (Blais, 1999). The inspection records for 3,419 buildings were obtained in the Simi Valley area and were removed from the database. The 58,601 remaining inspection records were analyzed.

Different types of information were available for various portion of the 58,601 inspection records. For example, tag records were available for 58,364 of the inspection records. The number of stories were recorded in 50,154 inspections. The types of buildings (e.g., timber, concrete block, steel frame, etc.) and year of construction were available from 52,449 and 52,776 inspection records, respectively.

The records for 47,378 buildings were associated with one and two-story timber structures, principally single and multiple family residences. The database does not include specific information about the type of damage to each structure.

Fig. 1 shows the portion of the residential buildings most seriously affected by the Northridge earthquake superimposed on the topography of the San Fernando Valley area. The inspection records include location, type of tag, and/or damage estimate in dollars, and estimate of damage as a percentage of replacement cost. The tag records of 58,364 buildings were available.

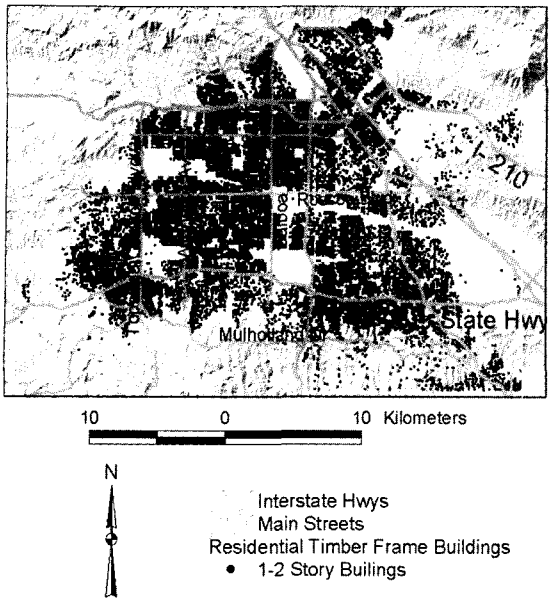


Fig. 1. Residential timber-frame buildings in San Fernando Valley Areas

Fig. 2 shows the spatial distribution of the residential buildings according to tags. The buildings with red tags were heavily concentrated in the Santa Monica Mountain area, which was subjected to landslide activity during the Northridge earthquake. The buildings with yellow and green tags were widely distributed over the area. Fig. 3 shows the buildings with green tags are 88% of inspected buildings. The remaining 10% and 2% of inspected buildings are associated with yellow and red tags, respectively.

Additional information from the inspection records, which includes number of stories, year built, and type of structure, was obtained from Eguchi and Huyck (2001). The 50,154 inspected buildings were categorized according to number of stories as shown in Fig. 4. The figures show that 99% of the residential buildings were only one story tall.

A total of 52,449 inspected buildings were categorized according to type of construction, including steel frame, reinforced concrete frame, concrete block or poured in place concrete, and timber frame. Fig. 5 shows that 97% of the buildings were timber frame construction, with the remaining 3% consisting of concrete or reinforced concrete and steel frame structures.

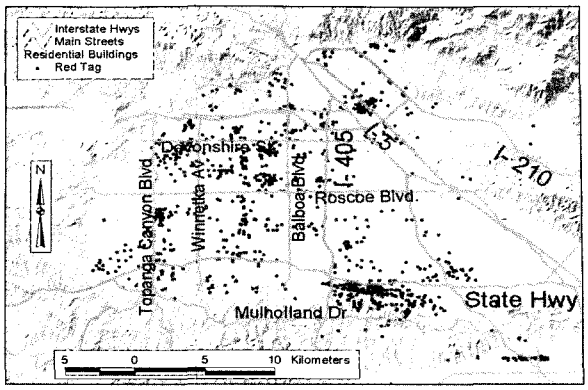


(a) red tag

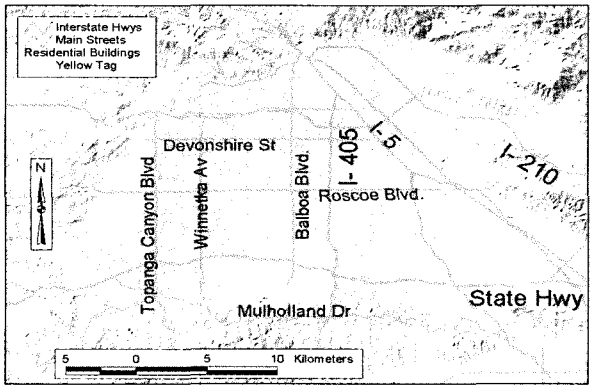


(b) yellow tag

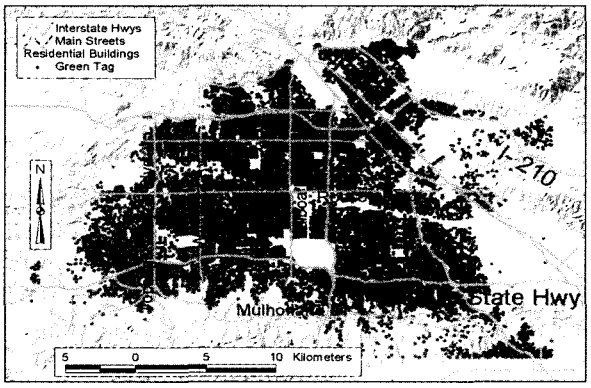


(c) green tag

Fig. 2. Spatial distribution of residential buildings according to inspection tag

The year of construction for 52,776 inspected buildings is shown in Fig. 6. The year represents the mid range value of each ten-year interval. Thirty-seven percent of the residential buildings were constructed in between 1950 and 1960. About one half of the residential structures were built after 1960.

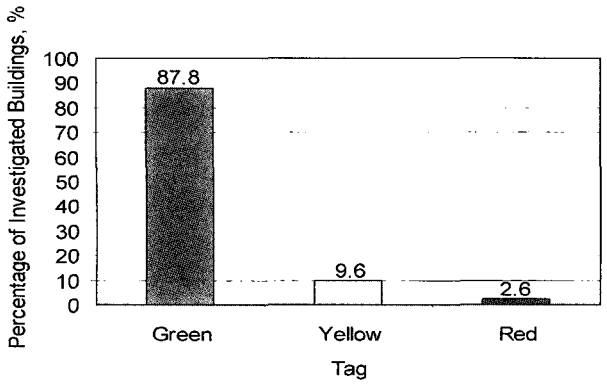


Fig. 3. Percentage of investigated buildings vs. tag

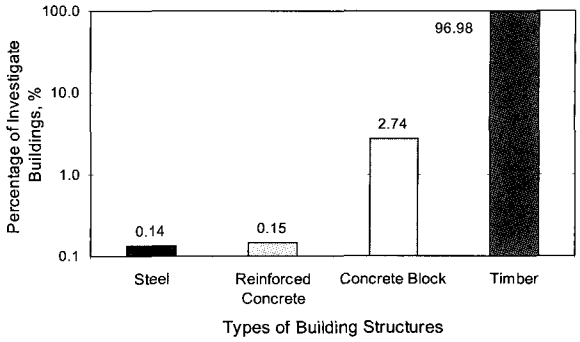


Fig. 5. Percentage of investigated buildings vs. types of building structures

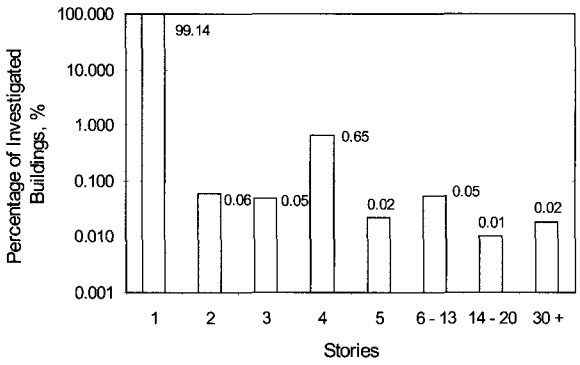


Fig. 4. Percentage of investigated buildings vs. the number of stories of the investigated buildings

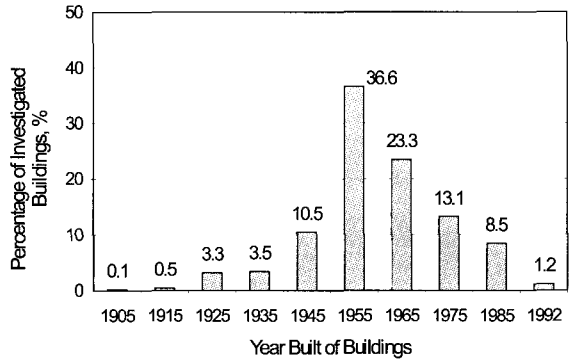


Fig. 6. Percentage of investigated buildings vs. year built of buildings

## 5. Loss Estimation Regressions

Two damage parameters, referred to as damage ratio and damage factor, were calculated with the database. Damage ratio is the fraction or % of existing structures with damage equal to or exceeding a particular damage factor. Damage factor is damage expressed as a % of building replacement cost.

The number of residential timber structures was geocoded at the center of each 0.65 km × 0.65 km cell in the GIS database. Fig. 7 shows the GIS grid superimposed on the spatial variation of peak ground velocity determined from 164 strong motion records geocoded as part of this study. By using a grid in which each cell is characterized by various damage ratios linked with damage factors, linear regressions can be performed to quantify damage vs. seismic parameters for loss estimation purposes.

Figs. 8 (a) and (b) show the linear regression of damage ratio (DR) vs. peak ground velocity (PGV) and Spectrum Intensity (SI) for various damage factors (DF). Most regressions for PGV show excellent fits as indicated by high $r^2$, although the "goodness" of fit is relatively low for DF ≥ 70%. In contrast, all regressions for SI have high $r^2$ and excellent characteristics with

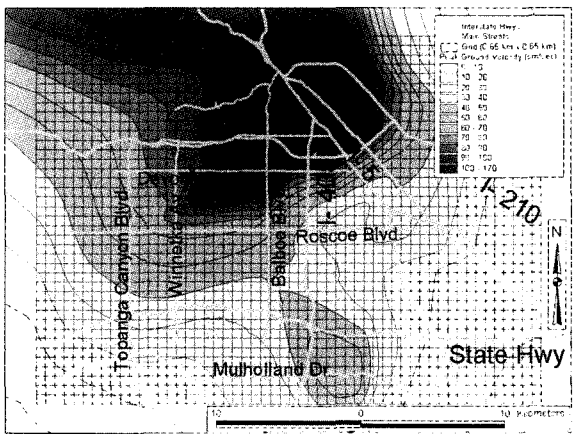


Fig. 7. GIS grid with tax assessor data superimposed on peak ground velocities

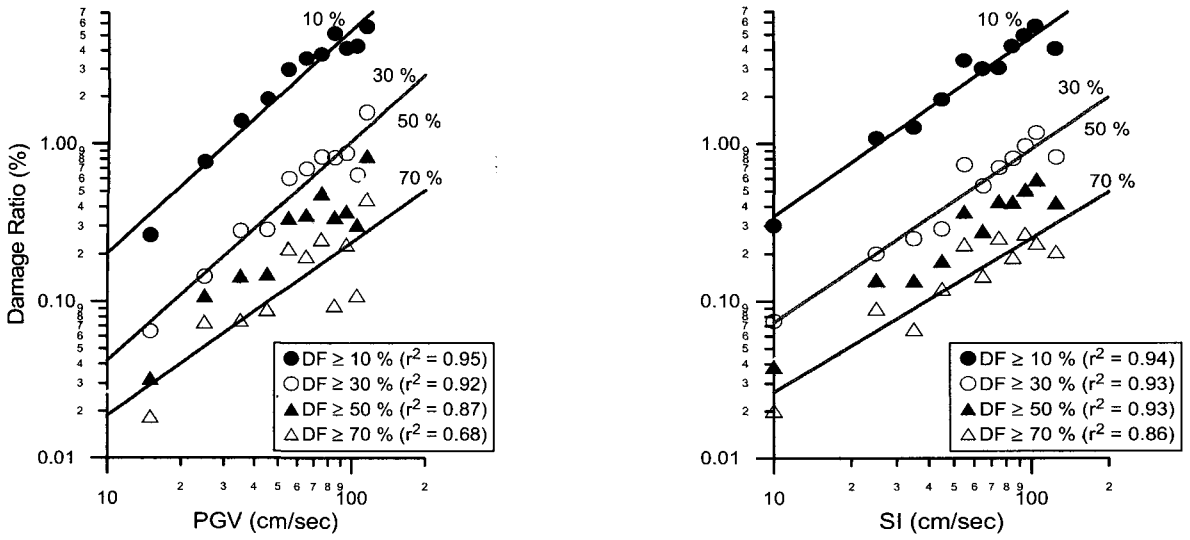


(a) (b)

Fig. 8. Damage ratio regressions for peak ground velocity (PGV) and spectrum intensity (SI) for 1-2 story timber frame buildings

respect to residuals. The relationships between damage and various seismic parameters were probed in this way to determine which parameters were statistically most significant as damage predictors. The seismic parameters investigated include the measured peak ground acceleration, velocity, and displacement; spectral acceleration and velocity for periods of 0.3 and 1.0 s; Arias Intensity; and SI.

SI is defined as the weighted average pseudo-velocity, SV, from the response spectra curve for a damping ratio, $\xi$ of 20% between periods, T, of 0.1 and 2.5 s:

$$SI = \frac{1}{2.4s} \int_{0.1}^{2.5} SV(T, \xi)\, dT \qquad (1)$$

SI was first proposed by Housner (1959) as a measure of the maximum stresses that would be induced in elastic structures by ground motion. Katayama et al. (1988) found that house damage correlated more strongly with SI than with peak acceleration, and recommended that SI calculations be performed for $\xi$ = 20%.

Fig. 9 shows the linear regression between DR and DF. Each DR in this plot applies for all timber structures recorded at particular DF. It is independent of the PGV, SI, or other seismic parameters measured at the locations of the structures. There is a remarkably close statistical fit of the regression line to the data, indicating a strong inverse correlation of DR with DF. Damage ratio

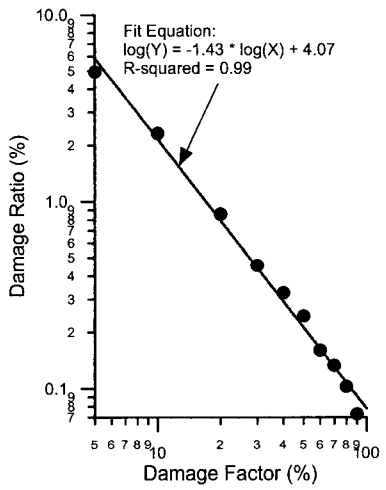


Fig. 9. Damage ratio vs. damage factor

decreases by an order of magnitude per similar increase in DF.

An examination of Fig. 8 reveals that DR, DF, and seismic parameter, SP, are interrelated in a consistent way. Using multiple linear regression techniques, this interrelationship can be expressed as:

$$\mathrm{Log_e}\ DR = \mathrm{Log_e}\ K + \alpha\ \mathrm{Log_e}\ SP - \beta\ \mathrm{Log_e}\ DF \qquad (2)$$

in which K is constants. Eq. (2) can be rewritten as:

$$DR = K(SP/DF^{\alpha/\beta})^{\alpha} \qquad (3)$$

in which $(SP/DF^{\alpha/\beta})$ is the scaled seismic parameter and $\alpha$ and $\beta$ are constants.

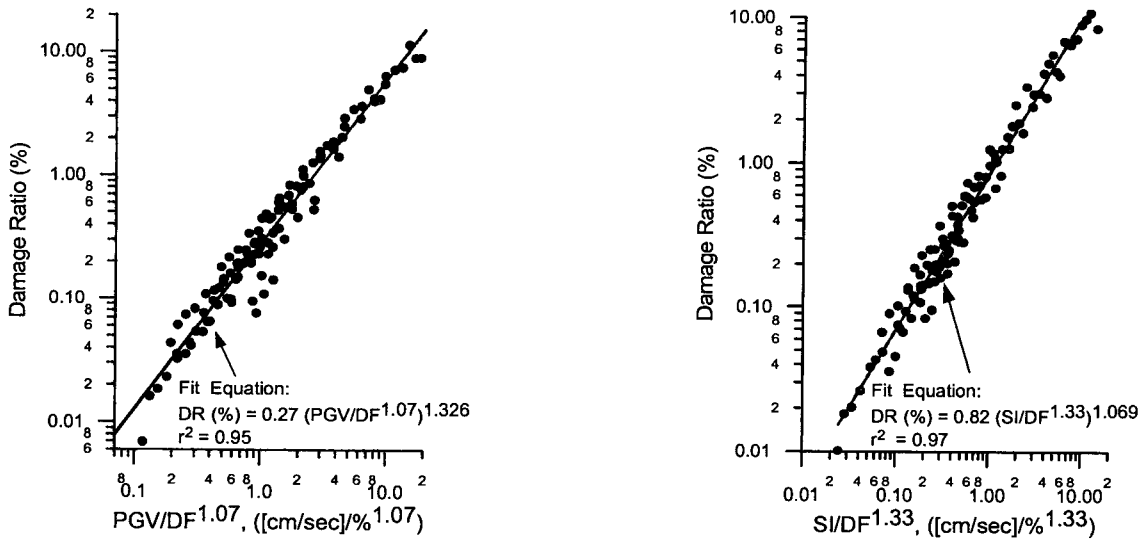


Fig. 10. Damage ratio regression for scaled PGV and SI for 1-2 story timber frame buildings

Using Eq. (3), the data in Figs. 8 (a) and (b) are replotted in Figs. 10 (a) and b as linear regressions that account for DR, DF, and SP. As evinced by high $r^2$ and excellent characteristics with respect to residuals, the relationships in Figs. 10 (a) and (b) are statistically significant.

Seismic parameters normalized with respect to DF combine the effects of strong motion and damage level in a convenient way that facilitates loss estimation. For example, consider an area for which the predicted SI is 30 cm/sec. Using the equations in Fig. 10 (b), the % of timber structures in that area that would have damage equal to or exceeding 10% of the building replacement cost is calculated as $DR = 0.82(30/10^{1.33})^{1.069}$, or 1.17%. For damage equal to or exceeding 50% replacement cost, $DR = 0.82(30/50^{1.33})^{1.069}$, or 0.11%.

## 6. Damage Pattern Recognition

With GIS, the spatial distribution of damage can be analyzed by dividing any map into cells, each of which is n by n in plan. Normalized damage, such as DR or pipeline repairs per km, is determined for each cell. Contours of normalized damage can then be drawn using the grid of equi-dimensional, n-sized cells. Previous research on water pipeline damage caused by the Northridge earthquake (O' Rourke and Jeon, 2000) has shown that a hyperbolic relationship exists between the threshold area coverage (TAC) [the fraction of the total representative map area within contours of normalized damage exceeding the overall average repair rate] and the dimensionless grid size, defined as the square root of $n^2$, the area of an individual cell, divided by the total map area, $A_T$.

Using the same concepts that were applied to the spatial distribution of pipeline damage, investigations were undertaken to define a relationship between TAC (defined for buildings as the fraction of the total map area within contours of DR exceeding the overall average DR) and the dimensionless grid size. The area selected for these investigations is shown in Fig. 11, where a grid of 24 × 36 cells is superimposed on a GIS map of the San Fernando Valley showing the locations of residential timber structures damaged by the Northridge earthquake. This grid is positioned such that timber structures are well distributed throughout the area covered by the grid. Accordingly, there are no significant zones within the covered area where timber structures, and therefore damaged structures, are absent.

The grid of 24 × 36 cells was chosen so that grids of successively larger cell sizes, covering the same area, could be created for n by n, 2n by 2n, 3n by 3n, 4n by

4n, 6n by 6n, 12n by 12n cells (where n = 0.65 km). The data generated for these grids and various DFs are plotted in Fig. 12. The inset diagram in Fig. 12 illustrates the concepts of TAC and DGS. The sum of the map areas within the overall average DR contour lines ($A_1+A_2$) is expressed as a fraction of the total map area ($A_C$) for which the generation of contour lines is valid. The contour lines were generated with ARC Info software (ESRI, 1994) that utilizes a Triangulated Irregular Network procedure with bivariate quintic interpolation.

All relationships are well described by hyperbolic functions, similar to the hyperbolic function that represents pipeline damage (O'Rourke and Jeon, 2000). Because building damage is characterized by DF, it has an additional dimension when compared to the single hyperbolic curve for pipelines. In fact, Fig. 12 is actually a hyperbolic surface for which the initial slopes and asymptotes vary as a function of DF.

Experience has shown that the ideal TAC for visualization is about 0.33. Fig. 12 indicates that the dimensionless grid size to achieve this TAC varies significantly, depending on DF.

Fig. 13 illustrates the application of Fig. 12 for damage intensity recognition and computer "zooming". The top map shows the entire San Fernando Valley and adjacent areas. The figure shows a cascade of different computer screens that "zoom" on increasingly smaller areas from top to bottom. Each screen shows as blue dots the actual locations of one to two story timber frame structures with DF $\geq$ 70% after the Northridge earthquake. The red contour lines indicate areas of highest damage intensity.

The contour lines in the top map were generated by analyzing the data with a GIS grid size chosen for TAC = 0.33 from Fig. 12. The area outlined in red in the top map was identified for more detailed assessment. The grid size for this assessment was again determined for TAC = 0.33 from Fig. 12. The map in the center of the figure shows an expanded view of the area outlined above after computer analysis. The zones of highest damage intensity for this new map are surrounded by red contour lines.

A similar procedure was followed for the center map in which an area for more detailed assessment was identified within the outline of the map at the top of the figure. The map at the bottom of the figure shows an expanded view of this new area in which the areas of greatest damage intensity are again surrounded by the contour lines of the map at the middle of the figure.

Because the relationships in Fig. 12 are independent of scale, the same algorithm for a specific DF can be used for increasingly smaller portions of the original map to "zoom" on areas of most intense damage. The visualization algorithm allows personnel who are not specifically knowledgeable about structures or trained in pattern recognition to identify the locations of most severe damage for allocation of aid and emergency

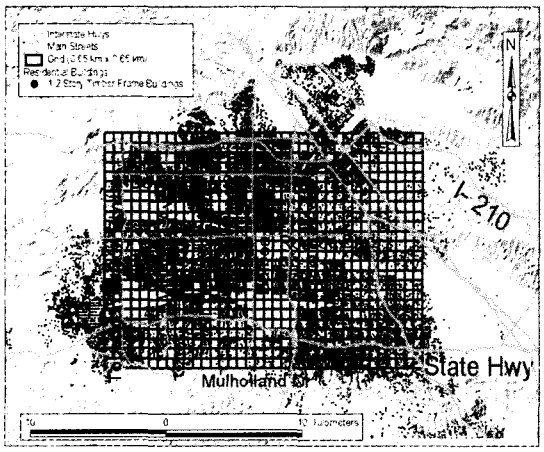


Fig. 11. GIS grid with tax assessor data superimposed on maps with 1-2 story timber frame buildings

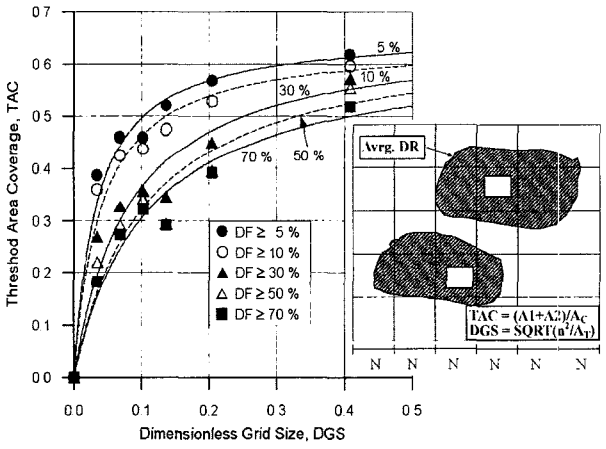


Fig. 12. Hyperbolic fit for threshold area coverage and dimensionless grid size for 1-2 story timber frame

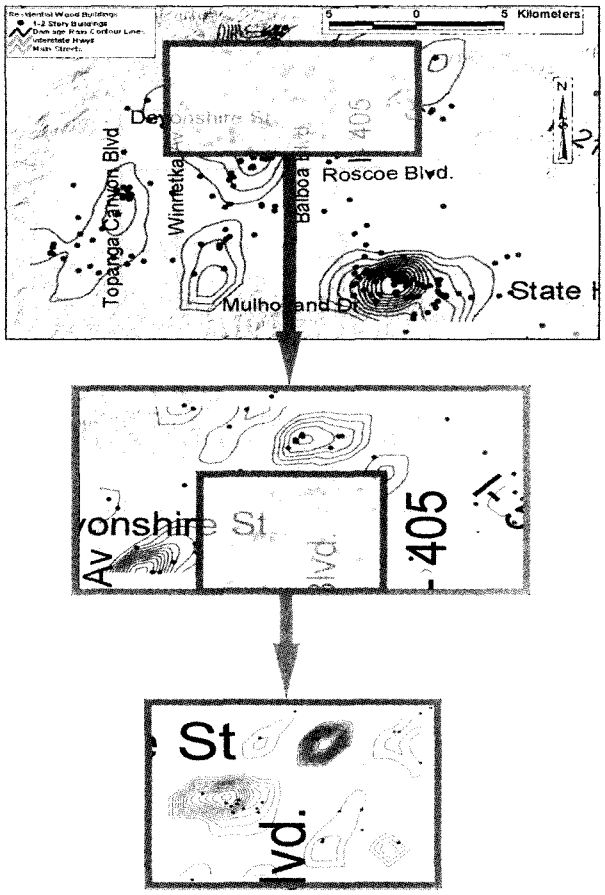


Fig. 13. TAC analysis for building DF 70%

services.

The entire process is easy to computerize, and personnel would be able to outline any part of a map with a "mouse" and click on the area so defined. In each instance of defining a smaller area for evaluation, the average DR is recalculated for the new, smaller-sized map. In this way the average is calibrated to each new map area.

When the damage pattern recognition algorithms are combined with regional data rapidly acquired by advanced remote sensing technologies, the potential exists for accelerated management of data and quick deployment of life and property saving services. By combining advanced remote sensing with the GIS pattern recognition process described in this work, advanced technologies are being expanded for a new generation of emergency response and rapid decision support systems.

## 7. Conclusions

Statistically significant regressions have been developed between the fraction of existing residential timber buildings at any damage state and the magnitudes of various seismic parameters. Such work improves loss estimation through GIS evaluation of spatially distributed damage.

GIS research on visualizing damage patterns in pipeline networks has been extended to buildings. Algorithms developed for pipelines have been modified and validated to choose optimal GIS mesh dimensions and contour intervals for identifying post-earthquake damage patterns in buildings to support rapid deployment of emergency services.

## Acknowledgements

The research described in this paper was supported through the Multidisciplinary Center for Earthquake Engineering Research (MCEER), Buffalo, NY and the National Science Foundation (NSF). Support for GIS visualization development was also provided by the Institute for Civil Infrastructure Systems (ICIS), New York, NY. Special thanks are expanded to Ron Eguchi and Charles Huyck of ImageCat, Inc., Long Beach, CA, for their assistance in acquiring and interpreting databases related to Northridge earthquake building damage.

## References

1. Akers, D. J. (1994), "Performance of Wood-Framed Structures in the January 17, 1994, Northridge Earthquake", Infrastructure: New Materials and Methods of Repair, *Proceedings, 3rd Materials Engineering Conference*, San Diego, CA, Nov.13-16, pp.662-668.
2. Applied Technology Council (1989), *Procedures for Post earthquake Safety Evaluation of Buildings*, ATC-20, Sanfrancisco, CA.
3. Blais, N. C. (1999), *Personal Communications*, EQE, Irvine, CA.
4. Comerio, M. C., Landis, J. D., Firpo, C. J., and Monzon J. P. (1996), "Residential Earthquake Recovery", California Policy Seminiar, Berkeley, CA.
5. Eguchi, R. T. and Huyck, C. K. (2001), *Personal Communication*, ImageCat, Long Beach, CA.
6. Eguchi, R. T., Goltz, J. D., Taylor, C. E., Chang, S. E., Flores, P. J., Johnson, L. A., Seligson, H. A., and Blais, N. C. (1996), "The Northridge Earthquake as an Economic Event: Direct Capital

Losses, Analyzing Economic Impacts and Recovery from Urban Earthquake: Issue for Policy Makers", *EERI Conference*, Pasadena, CA, October 10-11, pp.1-28.

7. ESRI (1994), "*The Arc/Info User's Guide*", Environmental Systems Research Institute, Inc., Redlands, CA.
8. Filiatrault, A. and Stieda C. K. A. (1995), "Seismic Weakness of Some Residential Wood Framed Buildings: Confirmations from the 1994 Northridge Earthquake", *Canadian Journal of Civil Engineering*, Vol.22, No.2, Apr., pp.403-414.
9. Housner, G. W. (1959), "Behavior of Structures During Earthquakes", *Journal of Engineering Mechanics Division*, ASCE, Vol.85, No.EM4, pp.109-129.
10. Jeon, S.-S. (2002), *Earthquake Performance of Pipelines and Residential Buildings and Rehabilitation with Cast-In-Place Pipe Lining Systems*, Ph.D. Thesis, Cornell University, Ithaca, NY.
11. Katayama, T., Sato, N., and Saito, K. (1988), "SI-Sensor for the Identification of Destructive Earthquake Ground Motion", *Proc. of 9th World Conference on Earthquake Engineering*, Vol.VII, Tokyo-Kyoto, Japan, August, pp.667-672.
12. Kircher, C. A., Reitherman, R. K., Whitman, R. V., and Arnold, C. (1997), "Estimation of Earthquake Losses to Buildings", *Earthquake Spectra*, Vol.13, No.4, pp.703-720.
13. MEGA-CITIES (2001), Anonymous ftp site: *http://www.megacities.org/network/losangeles.asp*
14. O'Rourke, T.D. and Jeon, S.-S. (2000), "Seismic Zonation for Lifelines and Utilities", *Proc. of 6th International Conference on Seismic Zonation*, Keynote Paper, EERI, Palm Springs, CA, pp.35.

(received on Mar. 2, 2004, accepted on Jul. 20, 2004)